Chapter 8

Aerosol–Cloud Interaction: A Case Study

Sandeep R. Varpe, Gajanan R. Aher,
Amol R. Kolhe and Sanjay D. More

Additional information is available at the end of the chapter

http://dx.doi.org/10.5772/65237

Abstract

MODerate Resolution Imaging Spectroradiometer (MODIS) retrieved aerosol and cloud products at the nine selected stations over Western Himalayan and Deccan Plateau regions were inferred to bring out their salient features and to investigate aerosol–cloud interaction. Annually, Ångström exponent (AE) decreases with aerosol optical depth (AOD) while in winter it increases with AOD at most of the stations. Results bring out positive and/or negative association between AOD and almost all the cloud parameters over the selected stations. Aerosol indirect effect (AIE) is quantified for fixed liquid water path (LWP) bins ranging from 1 to 350 g/m^2 at an interval of 25 g/m^2 for three categories of stations, viz., CAT-H, CAT-M, and CAT-L based on heavy, moderate, and low aerosol loading, respectively. AIE is negative at CAT-H (−0.04 ± 0.14), while it is positive at CAT-M (0.01 ± 0.07) and CAT-L (0.10 ± 0.48). During winter, negative AIE has been observed for all three categories. In pre-monsoon, the majority of LWP bins (86% at CAT-H and 60% at CAT-M) showed positive AIE, while about 71% of LWP bins indicted negative AIE at CAT-L. However, during monsoon about 63–71% of LWP bins showed negative AIE at these categories. Study elucidates the influence of factors like cloud type, cloud dynamics/thermodynamics on aerosol–cloud interactions.

Keywords: aerosol–cloud interaction, aerosol indirect effect, aerosol optical depth, Twomey-effect, liquid water path

1. Introduction

Atmospheric aerosols have been found to affect the earth's climate in many characteristic ways [1, 2]. They can affect the energy balance of the earth–atmosphere system by producing a direct or indirect change in the weather and climate system [3]. The direct interaction of aerosols

involves both scattering and absorption of radiation, and the relative importance of these processes depends on their chemical composition, refractive index, and size distribution [4, 5]. The indirect effect of aerosols on climate occurs by modifying the cloud optical properties [6]. Thus, the concentration, size, and composition of aerosols which can act as cloud condensation nuclei determine the cloud properties, evolution, and development of precipitation [7]. Aerosols modify cloud properties and precipitation via a variety of mechanisms with varying and contradicting consequences [8].

Cloud interactions with aerosols are hypothesized to be critical to understanding the climate change since clouds play a pivotal role in controlling incoming and outgoing radiation [9]. A large number of studies showed that the anthropogenic aerosols change clouds and their optical properties [4, 10, 11]. Atmospheric aerosols change the concentration and size of the cloud droplets which in turn lead to a change in cloud albedo, its lifetime and thereby affect the precipitation [6, 12]. Also, the reduction in cloud effective radius due to the increase in cloud droplet number concentration (CDNC) leads to the increase in cloud lifetime. The possible repercussion of this process is to decrease the rate of surface evaporation which results in stable and drier atmosphere as a result of the reduction in cloud formation [12]. Anthropogenic aerosols influence mixed-phase clouds in a number of ways and needs comprehensive study to understand the precise phenomenon. A great number of studies were conducted on the possible modification of cloud properties via the interaction with atmospheric aerosol particles, as this may lead to important changes in the Earth's climate. Biomass burning aerosols have been shown to affect clouds through both microphysical and radiative mechanisms [7, 13]. Biomass burning, from both deforestation and annual agricultural burning, is the largest anthropogenic source of such particles in the Southern Hemisphere. Biomass burning aerosols are hygroscopic and can serve as cloud condensation nuclei [14, 15]. More recently, satellite analyses have revealed a persistent correlation between cloud fraction and aerosol optical depth in regions influenced by marine aerosol, smoke, dust, and industrial air pollution [4].

The first indirect effect known as the Twomey effect produces the reduction in cloud effective radius due to the increase in aerosol loading for fixed liquid water path (LWP). Opposite of this effect (i.e., as aerosol loading increases cloud effective radius also increases) were observed over some parts of the world in certain environmental conditions [16]. The Twomey effect and Albrecht effect (i.e., lifetime effect) facilitate cooling of the atmosphere by increasing cloud optical depth (COD) and cloud fraction (CF), respectively [17]. This causes a reduction in the net solar radiation at the top of the atmosphere and hence at the surface. Several other studies have pointed out that the aerosol–cloud interactions are not determined by aerosols alone, but the regional meteorological conditions can play a significant role in this relationship [18]. Comparison of the modeled results and MODerate Resolution Imaging Spectroradiometer (MODIS) retrievals for aerosol indirect effect investigated by Myhre et al. [10] and Storelvmo et al. [18] showed a negative correlation between AOD and cloud effective radius (CER) while a positive correlation was observed between AOD and cloud optical depth (COD).

Extensive studies were conducted on various mechanisms of cloud properties through the interaction of atmospheric aerosol particles with cloud parameters which further influence the

http://dx.doi.org/10.5772/65237

earth's climate. It was found that at low AODs, cloud optical depth (COD) increases with increasing AOD while COD decreases with increasing AOD at higher AODs. This increase was attributed to a combination of microphysical and dynamical effects, while the decrease was due to the dominance of radiative effects that thin and darken clouds [19]. The AOD and cloud fraction correlation increases for those regions which have more particulate matter due to dust, biomass, industrial, and domestic activities [20].

In the present study, we have analyzed 11 years of MODIS aerosol and cloud products at the selected stations over Western Himalayan (75°E–80°E; 29°N–33°N) and Deccan Plateau (73°E–75°E; 16°N–19°N) regions. The selected stations over these regions comprised of (1) Dharmashala (DSL), (2) Mandi (MND), (3) Shimla (SML), (4) Ludhiana (LDN), (5) Patiala (PTL), (6) Muzaffarnagar (MZR), (7) Pune (PUN), (8) Satara (STR), and (9) Kolhapur (KPR) (abbreviated hereinafter as DSL, MND, SML, LDN, PTL, MZR PUN, STR, and KPR, respectively). Western Himalaya is desert dust dominated region while Deccan Plateau is dominated by fossil fuel and biomass burning. The study deals with the spatiotemporal variations of the MODIS retrieved aerosol and cloud products at the nine selected stations over Western Himalayan and Deccan Plateau regions to bring out their salient features. The data were also employed to investigate aerosol–cloud interaction and to quantify the aerosol indirect effect (AIE) over these regions.

2. Topography of study region

The Deccan Plateau is a large region that covers most of South Central India. The average elevation is 1000–2000 feet (305 and 610 m) above sea level along the northern sections of the region and 2000–3000 feet (610 and 915 m) in the southern section. Red loam or sandy loam soil usually overlies the granites and metamorphic rocks resulting in less fertile and less moisture retentive soil than found in the North Deccan region. The region slopes generally eastward allowing the drainage to flow toward the Bay of Bengal. Water in the rivers fluctuates considerably during the monsoon and the dry seasons. Their only source of water is the monsoon rains unlike rivers flowing out of the Himalayas that have year-round moisture from snow packs in the high mountains. In the winter or dry season, many of the rivers throughout the South Deccan become almost dry and are useless for irrigation. Also, some of the rivers flow through well-incised valleys, allowing little space for a flood plain and making it nearly impossible to direct water for irrigation onto the adjoining uplands. The climate is generally semi-arid with <35 inches (89 cm) of rainfall. Ironically, the Western Ghats are only 30–40 miles (48–64 km) away with annual precipitations exceeding 100 inches (254 cm).

In the Indian part of the Western Himalayas the surface weather elements, like precipitation and temperature, are intensely governed by local topography and local atmospheric circulations. The different altitude and orientation of the Himalayan ranges give rise to different thermo dynamical and dynamical forcing. Topography, heterogeneity, and land use variability are the characteristics of Western Himalayas (WH). Western disturbances (WDs), embedded in large-scale westerlies are responsible for winter precipitation, mainly snow, in WH. The

interplay of topography with WDs determines orographic precipitation over the Himalayan region.

3. Data products and methodology

Satellite observations have advantages over the ground-based measurements, in that, they provide information over the larger spatial domain [21]. The MODIS was designed with aerosol and cloud remote sensing in mind [22]. The MODerate Resolution Imaging Spectroradiometer (MODIS) aboard the Terra (launched in 1999) and Aqua (launched in 2002) monitors the earth–atmosphere system twice daily over a given location. It is sun-synchronous and near polar orbiting satellite with a circular orbit of 705 km above the surface. MODIS has 36 bands ranging from 0.4 to 14.4 μm wavelengths with three different spatial resolutions (250, 500, and 1000 m) and views the Earth with a swath of 2330 km, thereby providing near-global coverage on daily basis, with equatorial crossing local time of 10:30 am and 1:30 pm for Terra and Aqua, respectively (http://modis.gsfc.nasa.gov/).

Among the hundreds of products derived from MODIS-measured radiances are a suite of aerosol products [23] and another set of cloud products [24], including aerosol optical depth (AOD), cloud top pressure, and cloud fraction. Often, the AOD is used as a proxy for the cloud condensation nucleus (CCN) concentration. The reliability of this proxy depends on the uniformity of the aerosol size, composition, vertical distribution, but may in many cases be used as a first approximation. The MODIS data are available at different processing levels, level 1.0 (geolocated radiance and brightness temperature), level 2.0 (retrieved geophysical data products) and level 3.0 (gridded points) [24]. MODIS uses infrared bands to determine the physical properties of cloud in relation to cloud top pressure and temperature, and visible and near-infrared bands to determine optical and microphysical cloud properties [23, 25]. For water vapor, the retrieval the near-infrared region is adopted.

For this study, simultaneously retrieved datasets from MODIS (Terra) for the period 2000–2010 were used. Terra MODIS level_3 (C_005) monthly data products of aerosol optical depth (AOD), Ångström exponent (AE), cloud fraction (CF, day), water vapor (WV, above cloud), cloud effective radius (CER, liquid), liquid water path (LWP), and cloud optical depth (COD, liquid) were retrieved over the study region. As shown in **Figure 1**, the study regions were divided into 1° × 1° grid box centered at (1) DSL (32°16′ N; 76°23′E), (2) MND (31°43′ N; 76°58′ E), (3) SML (31°06′ N; 77°13′ E), (4) LDN (30°55′ N; 75°54′E), (5) PTL (30°20′ N; 76°25′ E), (6) MZR (29°28′ N; 77°44′E), (7) PUN (18°31′ N; 73°55′ E), (8) STR, (17°42′ N; 74°02′ E), and (9) KPR(16°42′ N; 74°16′ E).

For the estimation of aerosol indirect effect (AIE) on the basis of the observed AODs, we grouped the selected stations into different categories viz., CAT-H (heavy aerosol loading), CAT-M (moderate aerosol loading), and CAT-L (low aerosol loading). The MODIS (Terra) level_3 (C_005) daily data products of AOD, LWP, and CER were retrieved for this estimation, and analysis was performed over each category and as well as over each station keeping the fixed LWP constraint. The retrieved LWP and CER were divided into 14 different bin sizes.

http://dx.doi.org/10.5772/65237

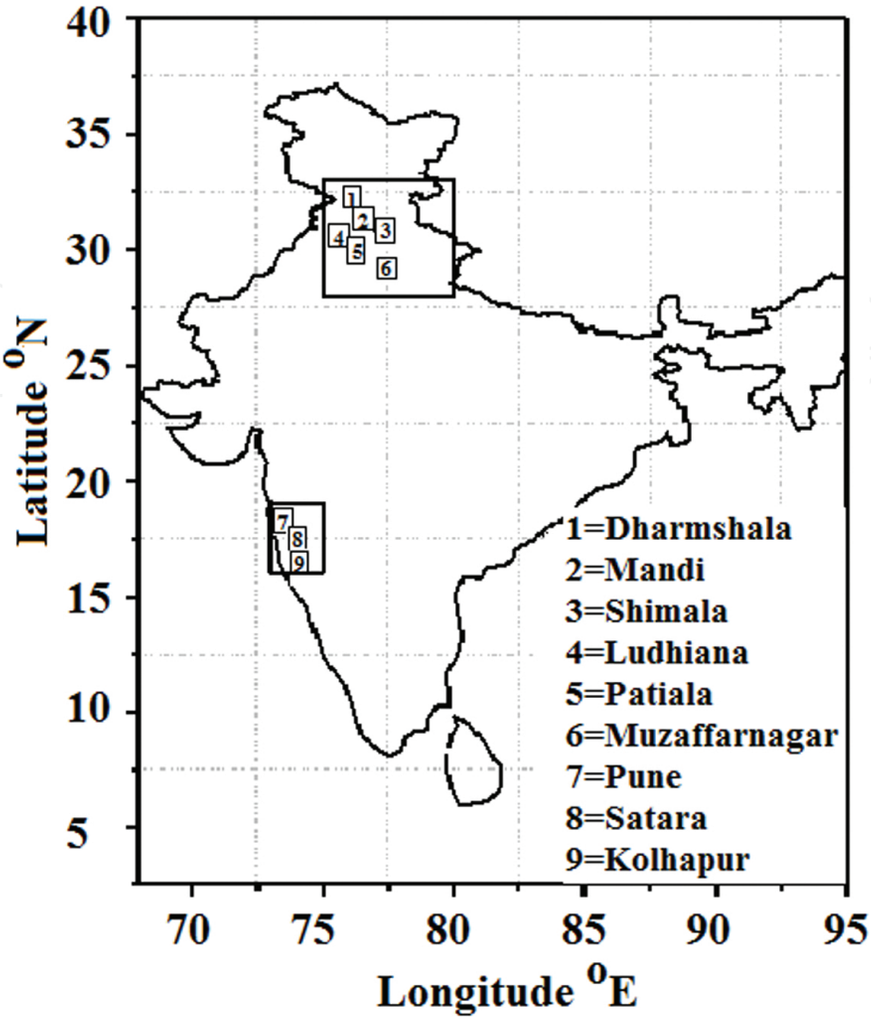

Figure 1. Study regions selected based on the dominant aerosol sources over India.

AIE was estimated for different seasons and for the entire study period 2000–2010 by evolving a linear least square fit to the plot between CER and AOD at fixed LWP and using the following equation [26],

$$\mathrm{AIE} = -\frac{d \ln r_e}{d \ln \tau_a} \tag{1}$$

Here, r_e is the cloud effective radius (CER) for fixed LWP and τ_a is the AOD. The degree of significance of AIE and correlation coefficients of linear regression fit has been also determined over the selected stations using two-tailed t-tests at 90 and 95% of confidence level. The correlation coefficients between AOD and other parameters (AE, CF, COD, CER, LWP, and WV) for 11 years data at each station are given in **Table 2**, and seasonal correlations of these parameters are given in **Table 3**. In these tables, the doubly underlined correlation coefficients are significant at 0.05 level (95% confidence level) while singly underlined correlation coefficients are significant at 0.1 level (90% confidence level) and the rest are less significant.

4. Results and discussion

4.1. Spatial climatology of aerosol optical depth

The spatial distribution of the monthly mean AODs for the period 2000–2010 at a wavelength 550 nm has been derived and is plotted in **Figure 2**. It reveals that the aerosol loading (i.e., AOD) have considerable influence on the atmosphere over Western Himalayan, Deccan Plateau regions, and their associated stations viz., DSL, MND, SML, LDN, PTL, MZR, PUN, STR, and KPR. The spatial distribution of AOD depicts occurrence of consistently high AODs (~0.7) over the Western Himalaya. It was found that the long-range transport of desert dust from the Arabian Peninsula contributes to the net regional aerosol loading with the marked increase in AOD over the Himalayan region in pre-monsoon months [27]. Over the Himalayan region, dust transport reaches up the slopes of the Himalayas and is further vertically elevated to higher altitudes because of the strong westerly pre-monsoon winds coupled with enhanced convection and pressure gradient resulting from large topographic differences [27]. High AODs have also been observed over the Ganga basin, situated in the Northern part of India [28]. The prevalence of high AODs over the Northern India is attributed to dense population density, the presence of heavy industries in the region, and the transport of desert dust from the nearby the Thar Desert in Rajasthan [29–31]. The spatial gradient of AOD shows an increase from the southern part of the Indian subcontinent to northern part up to the Himalayas [28]. Comparatively, AOD values over Deccan Plateau region (~0.35 to 0.4) are lower than WH region which can attribute to the anthropogenic activities, like the industrial region [32].

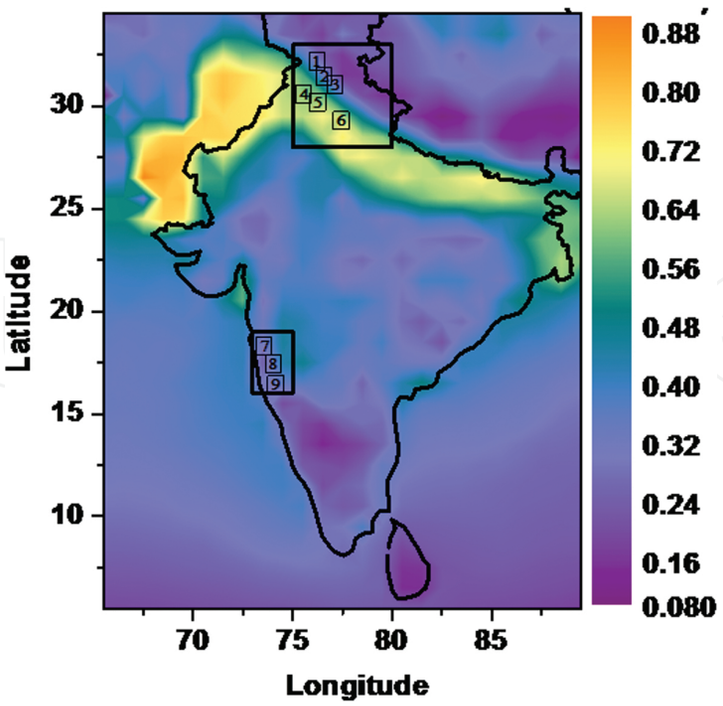

Figure 2. Spatial variation of monthly mean $AOD_{550\,nm}$ during 2000–2010.

http://dx.doi.org/10.5772/65237

4.2. Seasonal variation of AOD

The mean seasonal variation of $AOD_{550\ nm}$ wavelength was derived by considering MODIS (Terra) retrieved AODs over Western Himalayan and Deccan Plateau regions (i.e., stations associated with these regions) for the period of study. The resulting mean seasonal variation of AOD, for the period 2000–2010, elucidated in **Figure 3**, reveals a statistically significant seasonal variation of AODs during monsoon and other seasons. The seasonal mean AODs, given in **Table 1**, show that AOD was lowest during winter (0.29 ± 0.05) and highest during monsoon (0.60 ± 0.25) followed by pre-monsoon (0.42 ± 0.10) at all the stations. Higher AODs during the monsoon may be because of the hygroscopic growth of water-soluble aerosols and transport of larger sized aerosols (dust and sea salt) during favorable wind conditions [29]. Also, the ensemble mean monsoon AOD may be high due to limitations on the numbers of data points which were very few, because of the prevalence of overcast conditions (cloudy in nature) during most of the days. The similar increase in AOD during pre-monsoon and monsoon season has previously been reported for Indian Subcontinent [28].

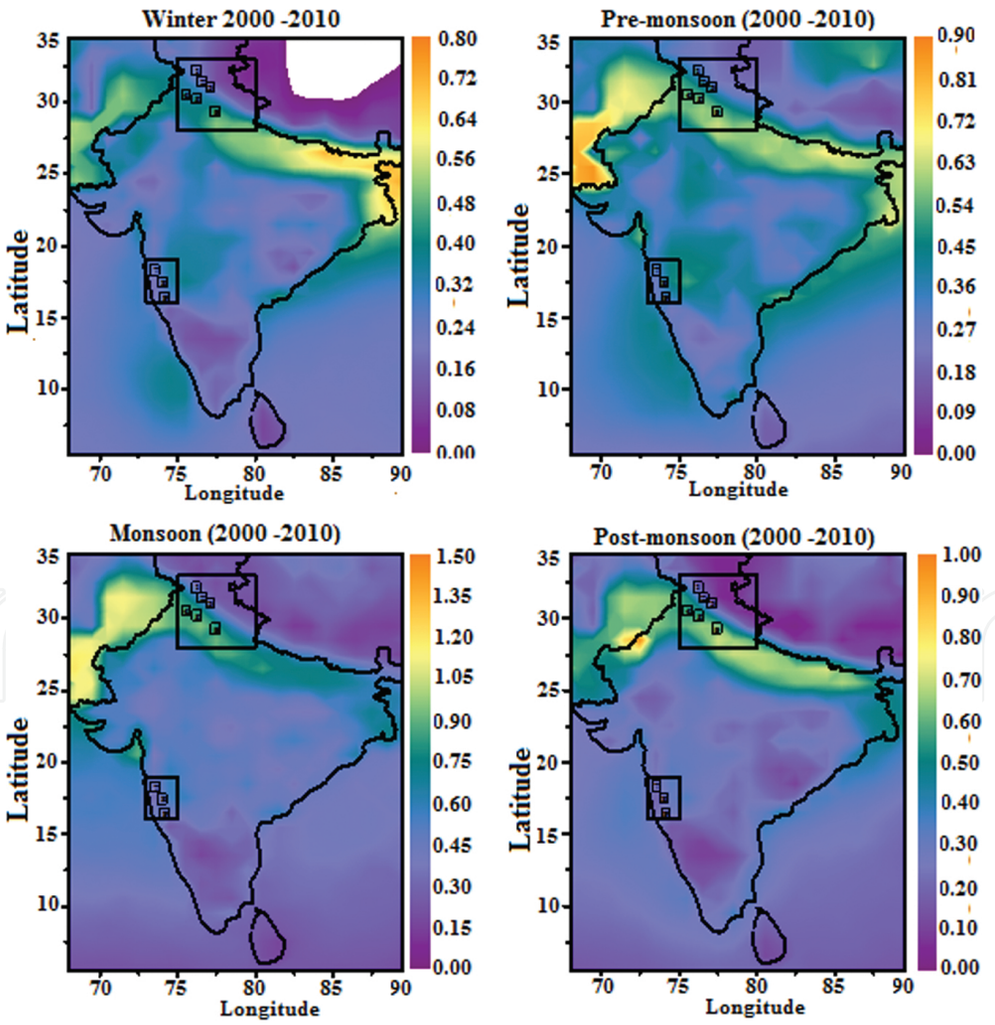

Figure 3. Seasonal variation of MODIS retrieved $AOD_{550\ nm}$ during the period 2000–2010.

Station wise, LDN, PTL, and MZR in Western Himalayan region depict higher mean AODs over the period 2000–2010 as compared to the other investigated cities viz., PUN, STR, and KPR in Deccan Plateau region. AODs at LDN, PTL, and MZR in pre-monsoon were found to be 0.53, 0.51, and 0.54, respectively, whereas the corresponding winter AODs at these places were found to be 0.35, 0.34, and 0.45, respectively. On the other hand, over PUN, STR, and KPR stations, AODs were found to be 0.30, 0.36, and 0.32, respectively, in pre-monsoon and 0.24, 0.26, and 0.23, respectively, during winter. Analysis indicates that the AODs generally increase from lower latitude to higher latitude [32]. The occurrence of high AODs at LDN, PTL, and MZR is due to their close proximity to the Thar Desert where frequent dust storms occur during pre-monsoon months. In addition, the presence of higher temperatures tends to hold more water vapor favoring aerosols to grow in size causing higher AODs at these sites. Aerosol loading over the studied region is low after the monsoon season as rainfall washes out most of the aerosol concentration [33]. The post-monsoon season shows a continuation of the trend observed for AOD distribution in winter.

Stations	Seasonal mean AOD and standard deviation			
	Winter	Pre-monsoon	Monsoon	Post-monsoon
Dharmashala	0.25 (±0.04)	0.37 (±0.11)	0.51 (±0.19)	0.31 (±0.07)
Mandi	0.22 (±0.04)	0.36 (±0.13)	0.49 (±0.20)	0.26 (±0.07)
Shimla	0.23 (±0.03)	0.37 (±0.11)	0.51 (±0.20)	0.28 (±0.07)
Ludhiana	0.35 (±0.05)	0.53 (±0.17)	0.86 (±0.37)	0.55 (±0.14)
Patiala	0.34 (±0.06)	0.51 (±0.16)	0.81 (±0.34)	0.51 (±0.13)
Muzaffarnagar	0.45 (±0.07)	0.54 (±0.17)	0.82 (±0.30)	0.70 (±0.14)
Pune	0.24 (±0.05)	0.30 (±0.05)	0.43 (±0.23)	0.24 (±0.06)
Satara	0.26 (±0.06)	0.36 (±0.05)	0.51 (±0.24)	0.25 (±0.05)
Kolhapur	0.23 (±0.06)	0.32 (±0.06)	0.46 (±0.20)	0.25 (±0.05)

Table 1. MODIS (Terra) derived mean seasonal AODs at the selected stations over Western Himalaya and Deccan Plateau Region during 2000–2010.

4.3. AOD and Ångström exponent (AE) correlation

Figure 4 shows the monthly mean composite plots of AOD and AE (α) for the selected stations in the Western Himalayan and Deccan Plateau regions during 2000–2010. Also, **Table 2** displays the correlation coefficients of linear regression analysis between AOD and AEs. It is clear from both **Table 2** and **Figure 4** that the MODIS retrieved AODs and AEs are either inversely or positively correlated and the correlations are significant at 95% confidence level at all the locations. It can be noticed that during monsoon season, AE is negatively correlated with AOD with 95% confidence level while in winter it shows positive correlations with AOD at all the stations. The positive correlation of AE with AOD was observed at the locations STR and KPR during pre-monsoon and at MZR, PUN, and KPR during post-monsoon season. This

kind of behavior may be attributed to the hygroscopic growth of the aerosol particles producing a significant shift in aerosol size spectrum which in turn can substantially influence the magnitude of the Ångström exponent. More particularly, the change in the ratio of small to large particles can also bring about a change in the Ångström exponent. A dry particle of anthropogenic origin may have a Ångström exponent which is 60% higher than a particle with a growth factor of 1.6, which illustrates that hygroscopic growth, can substantially impact the Ångström exponent [10]. It may be possible that high AOD during pre-monsoon is due to the increase in the size of the humidified aerosols present near the cloudy area.

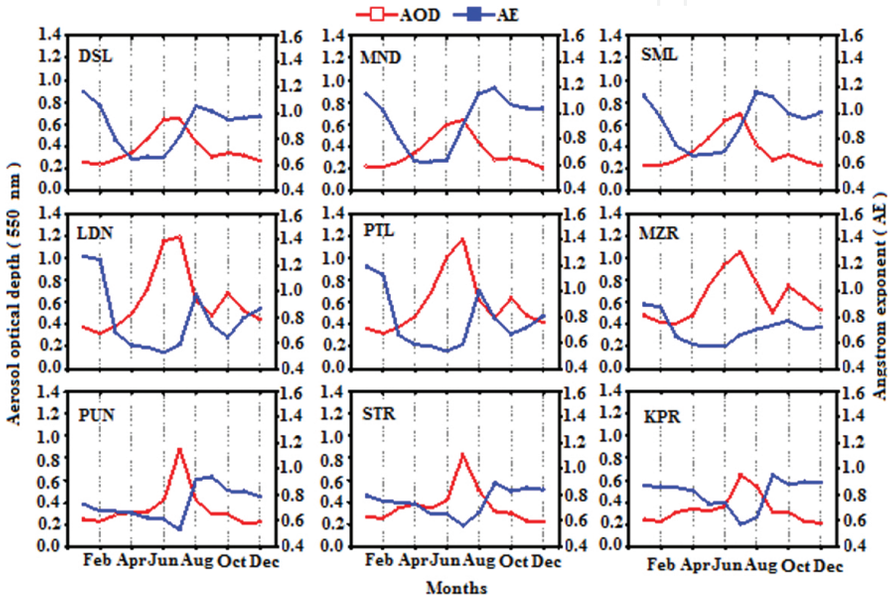

Figure 4. Monthly mean composite plots of AOD and AE over the selected stations in the Western Himalayan and Deccan Plateau regions during 2000–2010.

Stations	AE	CF	COD	CER	CWP	WV
DSL	**−0.48**	**0.53**	−0.07	**0.19**	0.09	**0.74**
MND	**−0.43**	**0.57**	0.12	**0.22**	**0.23**	**0.75**
SML	**−0.39**	**0.57**	0.02	**0.24**	*0.17*	**0.74**
LDN	**−0.54**	**0.60**	0.05	**0.19**	*0.16*	**0.66**
PTL	**−0.50**	**0.61**	0.03	**0.23**	0.14	**0.71**
MZR	**−0.31**	**0.54**	−0.03	**0.23**	0.09	**0.67**
PUN	**−0.26**	**0.57**	**0.34**	**0.19**	**0.43**	**0.37**
STR	**−0.60**	**0.60**	**0.40**	**0.33**	**0.48**	**0.37**
KPR	**−0.52**	**0.60**	**0.43**	**0.23**	**0.49**	**0.38**

Correlation coefficients bolded are significant at 0.05 level (95% confidence level), while italicized are significant at 0.1 level (90% confidence level) and the rest are less significant.

Table 2. Correlation coefficients of the linear regression analysis between AOD against AE and cloud parameters at each station for the period of 2000–2010.

The Ångström exponent is an approximate measure of the aerosol particle size distribution; smaller the Ångström exponent larger is the size of the particles [34]. **Figure 4** reveals that there is a decrease in Ångström exponent values with increase in the AODs at all sites. Higher values of α indicate a sharper aerosol size spectrum. It clearly shows the dramatic transformation in the aerosol spectra, from high accumulation mode domination during September through February months (revealed by values of $\alpha > 1.0$ and steep AOD spectra) to increased coarse mode domination ($\alpha < 1.0$) during March through June–July months. Lower values of AE clearly indicate that the dominance of coarse-mode aerosols which affirms the influx of transported coarse-mode dust aerosols from the Arabian Desert and the Thar Desert [31, 35].

4.4. Interaction between AOD and cloud parameters

The MODIS provides an enormous amount of data which is valuable for understanding how aerosols influence clouds [10]. Aerosols are highly variable in space and time with different properties, characteristics, and concentrations. It is this peculiar nature of aerosols along with prevailing the meteorological conditions that brings in a complicating factor and makes the aerosol–cloud interaction a complex phenomenon. Rain formation depends on the number concentration of aerosols in atmospheric pollution and is unaffected by low pollution; however, during heavy pollution episode, rainfall is significantly reduced. Aerosols act as ice nuclei and cloud condensation nuclei. The presence of small condensation nuclei in the atmosphere can initiate the suppression of heterogeneous freezing with the result that many small droplets remain liquid below the homogeneous freezing temperature [36]. However, most of the observational studies are based on specified cases from which it is difficult to determine as to which effects are more significant and dominant and thus their long-term implications remain unknown [37].

In the present work, an attempt has been made to understand and quantify the influential role of AOD on cloud parameters by analyzing correlations amongst them on spatial scale and by estimating AIE for the nine selected stations. The results are highlighted in the following subsections through the use of spatial correlation. In addition, we have estimated the seasonal correlation coefficients for each parameter at the selected stations as well as for the entire period of 2000–2010. The aerosol–cloud relationship has also been studied using the monthly mean composite plots for 11 years of data so used.

4.4.1. Influence of AOD on cloud fraction

The co-variation plot of $AOD_{550\ nm}$ and CF during the period 2000–2010 has been constructed over the selected nine sites in the Western Himalayan and Deccan Plateau region in India, and the results are displayed in **Figure 5**. Also, linear regression correlation coefficients for the plots of $AOD_{550\ nm}$ against AE and MODIS-retrieved cloud parameters viz., CF, COD, CER, CWP, and WV have been estimated for the selected time period of 11 years on a seasonal basis. The resulting data are shown in **Table 3** which reveals that the satellite retrieved cloud fraction data shows a strong positive correlation with $AOD_{550\ nm}$ at all the selected locations in the respective study regions. The present results are found to be consistent with those reported by Myhre et al. [10] and Kaufman et al. [4]. Interestingly, the correlation coefficients at heavy

columnar aerosol loading locations (AOD ranging between 0.59 and 0.65), i.e., LDN, PTL, and MZR and at relatively low columnar aerosol loading locations (AOD ranging between 0.31 and 0.36), i.e., PUN, STR, and KPR are more or less similar. It is important to note here that the Western Himalayan region is desert-dust dominated region due to its proximity to Thar Desert, whereas Deccan Plateau region is dominated by anthropogenic activity in the form of industrial/vehicular pollution and biomass burning. Consequently, the occurrence of higher correlations between $AOD_{550\ nm}$ and CF in these anthropogenically, biomass burning and desert-dust dominated aerosol regions indicate that the meteorological factors significantly influence this relationship [32]. Recently, it is found that the increasing aerosol concentration leads to increase in cloud cover and showing that the aerosol concentrations change the cloud properties [38]. This is because regions of low atmospheric pressure have more tendency to create conditions necessary for cloud formation by accumulating aerosol particles and water vapor [39].

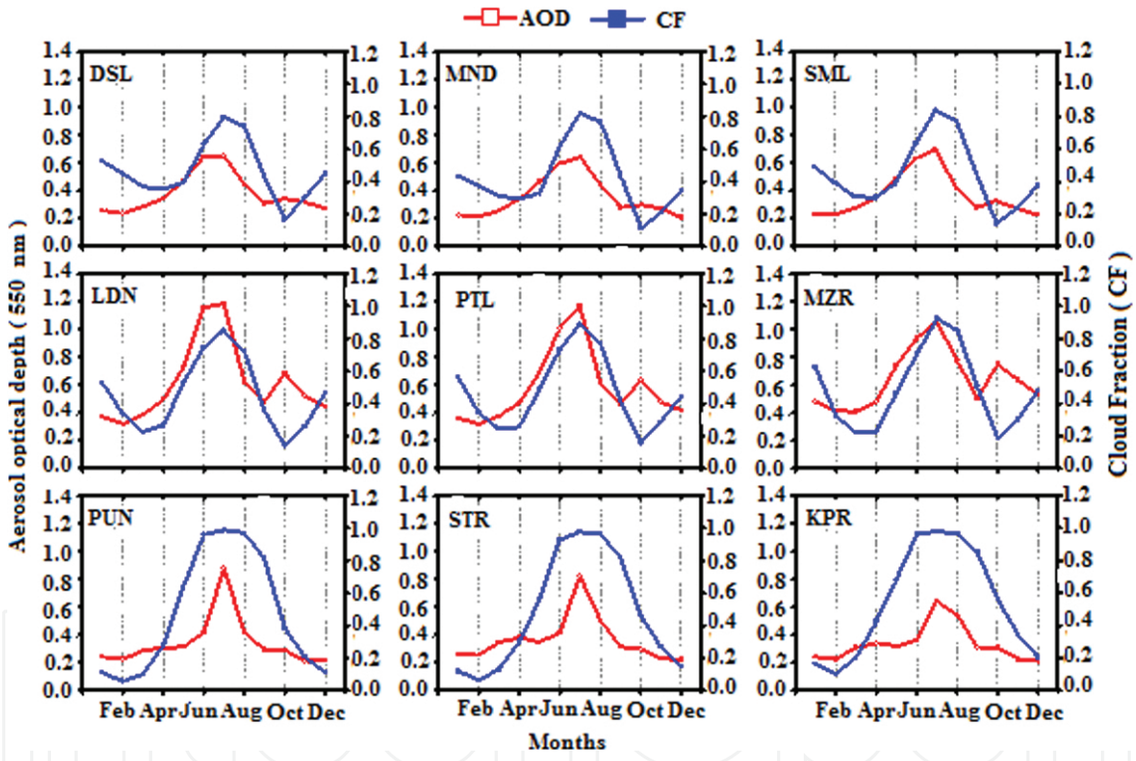

Figure 5. Monthly mean composite plots of AOD and CF at the selected stations in the Western Himalayan and Deccan Plateau regions during 2000–2010.

The monthly mean composite plots of AOD and CF during the period 2000–2010 (**Figure 5**) show that the CF increased with AOD at all locations throughout the entire period of study. The CF and AOD variations demonstrate an out of phase correlation during the winter season for the Western Himalayan stations. Also, the relationship becomes negative in the months of July and August as CF increased with a decrease in AOD. The magnitudes of the seasonal correlation coefficients between AOD and CF, given in **Table 3**, signify that the CF increases with AOD at all the station (except SML; negative correlations) during winter (DSL = 0.24,

MND = 0.14, LDN = 0.65, PTL = 0.47, MZR = 0.58, PUN = 0.42, STR = 0.65, KPR = 0.74), pre-monsoon (DSL = 0.31, MND = 0.34, LDN = 0.77, PTL = 0.74, MZR = 0.79, PUN = 0.30, STR = 0.10, KPR = 0.20) and monsoon(DSL = 0.51, MND = 0.49, LDN = 0.63, PTL = 0.61, MZR = 0.48, PUN = 0.46, STR = 0.53, KPR = 0.41) seasons. Myhre et al. [10] have found that the decrease of CF with increasing AOD occurs mainly for low AODs (below ~0.3) and also reported an increase in AOD with an increase in RH due to the swelling of hygroscopic particles which are near to the clouds. The cloud cover also exhibits a weak negative correlation with the potential temperature lapse rate, and vertical shear of the horizontal wind in the middle atmosphere [40]. This gives rise to shift in aerosol size distribution with smaller particles coming into optical range while larger particles moving out of it [41]. Positive correlations between CF and AOD appear to be the reflection of this effect. This increase may be due to the complexity of the domain, the type of land surface (albedo), the choice (classification) of aerosol mixtures applied in the MODIS retrieval for that particular area, the impact of meteorology on aerosol transport, and the aerosol chemistry. Kaufman et al. [4] mentioned that the cloud cover increases with increase in aerosol concentrations and found that the cloud properties change as a result of variations in large-scale atmospheric circulation and also affect aerosol concentrations. For example, regions of low atmospheric pressure are convergence zones that tend to accumulate aerosols and water vapor, thus generating conditions favorable for cloud formation [42].

Station	Parameters	Winter	Pre-monsoon	Monsoon	Post-monsoon
DSL	AE	0.215	**−0.580**	**−0.687**	−0.136
	CF	0.248	*0.316*	**0.519**	−0.184
	COD	0.285	**−0.344**	−0.058	−0.228
	CER	−0.184	−0.243	**−0.367**	0.317
	LWP	0.187	**−0.452**	−0.233	*−0.071*
	WV	0.243	**0.795**	**0.573**	**0.399**
MND	AE	0.106	**−0.589**	**−0.617**	−0.179
	CF	0.138	**0.345**	**0.494**	−0.274
	COD	0.295	−0.156	−0.027	−0.283
	CER	0.078	−0.140	−0.221	*0.330*
	LWP	0.259	−0.266	−0.141	−0.128
	WV	0.070	**0.774**	**0.598**	**0.466**
SML	AE	0.057	**−0.571**	**−0.659**	−0.192
	CF	−0.044	*−0.299*	**−0.342**	**0.406**
	COD	0.114	−0.157	−0.159	−0.212
	CER	−0.044	*−0.299*	**−0.342**	**0.406**
	LWP	0.116	−0.265	**−0.325**	0.004
	WV	0.274	**0.791**	**0.507**	**0.515**
LDN	AE	0.062	**−0.796**	**−0.607**	**−0.483**
	CF	**0.659**	**0.779**	**0.636**	**−0.361**
	COD	0.177	−0.057	0.205	−0.221
	CER	**−0.451**	−0.027	−0.122	0.220
	LWP	−0.077	−0.037	0.0596	−0.087
	WV	**0.577**	**0.855**	*0.262*	**0.445**
PTL	AE	0.122	**−0.750**	**−0.645**	**−0.352**

Station	Parameters	Winter	Pre-monsoon	Monsoon	Post-monsoon
	CF	**0.471**	**0.747**	**0.614**	**−0.371**
	COD	0.356	−0.104	−0.158	0.085
	CER	**−0.446**	−0.144	−0.238	**0.523**
	LWP	0.144	−0.123	**−0.331**	0.262
	WV	**0.596**	**0.848**	**0.449**	**0.378**
MZR	AE	0.172	**−0.686**	**−0.436**	**0.438**
	CF	**0.575**	**0.795**	**0.484**	−0.243
	COD	0.352	−0.108	−0.121	0.0099
	CER	**−0.634**	−0.280	−0.169	**0.392**
	LWP	−0.025	−0.168	−0.237	0.220
	WV	*0.383*	**0.851**	**0.493**	**0.481**
PUN	AE	**0.674**	−0.206	**−0.478**	0.165
	CF	*0.428*	*0.306*	**0.469**	**0.409**
	COD	−0.210	0.124	0.222	0.131
	CER	0.180	**−0.349**	**0.518**	−0.054
	LWP	−0.096	0.007	**0.320**	0.074
	WV	0.097	0.171	**−0.432**	*0.340*
STR	AE	**0.694**	0.113	**−0.628**	−0.136
	CF	**0.656**	0.100	**0.533**	**0.434**
	COD	−0.055	0.004	**0.364**	0.173
	CER	−0.323	−0.181	**0.400**	0.083
	LWP	−0.143	−0.132	**0.458**	0.195
	WV	0.127	−0.090	**−0.565**	*0.426*
KPR	AE	**0.704**	0.128	**−0.575**	0.049
	CF	**0.742**	0.206	**0.418**	**0.583**
	COD	−0.052	0.026	**0.389**	0.235
	CER	−0.260	−0.027	0.185	−0.105
	LWP	−0.159	−0.055	**0.430**	0.272
	WV	0.322	0.017	**−0.303**	*0.465*

Correlation coefficients bolded are significant at 0.05 level (95% confidence level), while italicized are significant at 0.1 level (90% confidence level) and the rest are less significant.

Table 3. Same as in **Table 2** but for different seasons during the period 2000–2010.

4.4.2. Association between AOD and cloud effective radius

The cloud effective radius (CER) is the weighted mean of the size distribution of cloud droplets in the atmosphere. CER (defined as the ratio of the third to the second moment of a droplet size distribution) is one of the key variables that are used for calculation of the radiative properties of liquid water clouds [43]. Analysis of the present data reveals that the CER and AOD values are positively correlated at all the locations during the study period 2000–2010 (**Table 2**). These findings are found to be consistent with the results of Yuan et al. [44] which manifested that the direct correlation between AOD and CER may be due to various artifacts as well as aerosol swelling, partial cloudiness, atmospheric dynamics, cloud three-dimensional (3D), and surface influence effects. Hygroscopic aerosols grow in size as a consequence of

moisture uptake from water vapor. The size and the refractive index of the aerosol change due to the hygroscopic growth of the aerosols resulting in the subsequent increase in AOD [26]. For example, aerosols which are in close proximity to the cloud swell more because of the higher moisture content present near the cloud producing larger AOD. Simultaneously, deeper clouds tend to have larger droplets than shallower clouds.

On the other hand, **Figure 6** shows that CER values are found to be lower in pre-monsoon months (0.4–0.6) and higher in monsoon months (0.8–1.3). Results clearly indicate that the Western Himalayan and Deccan Plateau regions receive maximum rainfall during the monsoon months. Bhawar and Devara [45] carried out the similar study over Pune and found that increase in CER produces an increase in COD which could result in more rainfall and *vice-versa*. The present results, on the seasonal scenario (shown in **Table 3**), also reveal that the CER is negatively correlated with AOD during winter and post-monsoon seasons at most of the stations. Analysis of the MODIS retrievals indicates that the negative/positive correlation of CER with AOD is not determined by aerosol–cloud interaction alone. Instead, the regional meteorological conditions, as well as aerosol type, clouds dynamics, and thermodynamics of the atmosphere, can play the significant role in this relationship.

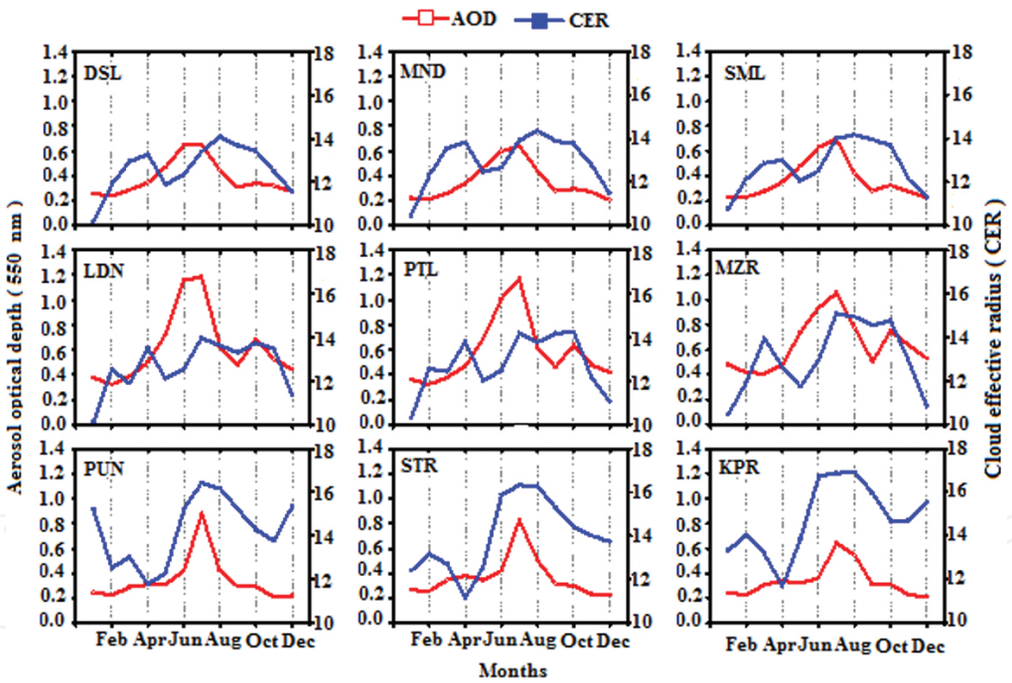

Figure 6. Monthly mean composite plots of AOD and CER at the selected stations in the Western Himalayan and Deccan Plateau regions during 2000–2010.

4.4.3. Effect of AOD on liquid water path

Results displayed in **Table 2** for the correlations between AOD and cloud parameters depict occurrence of relatively high positive correlations between AOD and LWP at PUN, STR, and KPR [correlation coefficient (R) ranging between 0.43 and 0.49] than that at DSL, MND, SML,

http://dx.doi.org/10.5772/65237

LDN, PTL, and MZR [correlation coefficient (R) ranging between 0.09 and 0.23] during 2000–2010. This indicates that the increase of LWP with AOD is consistent with the previous studies of Yuan et al. [44]. It suggests that the assumption, i.e., the first indirect effect is not always valid [44]. However, it should be noted that the MODIS LWP is not an independent measurement but estimated from the respective values of COD and CER.

Monthly variation of AOD and LWP for the study period (**Figure 7**) and their seasonal correlation analysis (**Table 3**) points out that the sign of correlation (negative/positive) changes from season to season and from place to place indicating spatiotemporal variability in these correlations. In winter, LWP decreases with increasing AOD at the stations LDN, MZR, PUN, STR, and KPR while it increases with AOD at DSL, MND, SML, and PTL. In pre-monsoon, at all the stations (except PUN), LWP was found to decrease as AOD increased. During monsoon, LWP decreases with AOD at stations DSL, MND, SML, PTL, and MZR while it increases with AOD at LDN, PUN, STR, and KPR. For the post-monsoon season, at the stations DSL, MND, and LDN, a negative relationship was observed between AOD and LWP while it was positive at the stations PTL, MZR, PUN, STR, and KPR. The possible reason behind the reduction of LWP during winter, pre-monsoon, monsoon, and post-monsoon seasons may be warming of clouds due to the dust aerosols, absorbing incoming solar radiation thereby increasing evaporation of cloud droplets leading to the reduction of LWP, i.e., the so-called semi-direct effect [46].

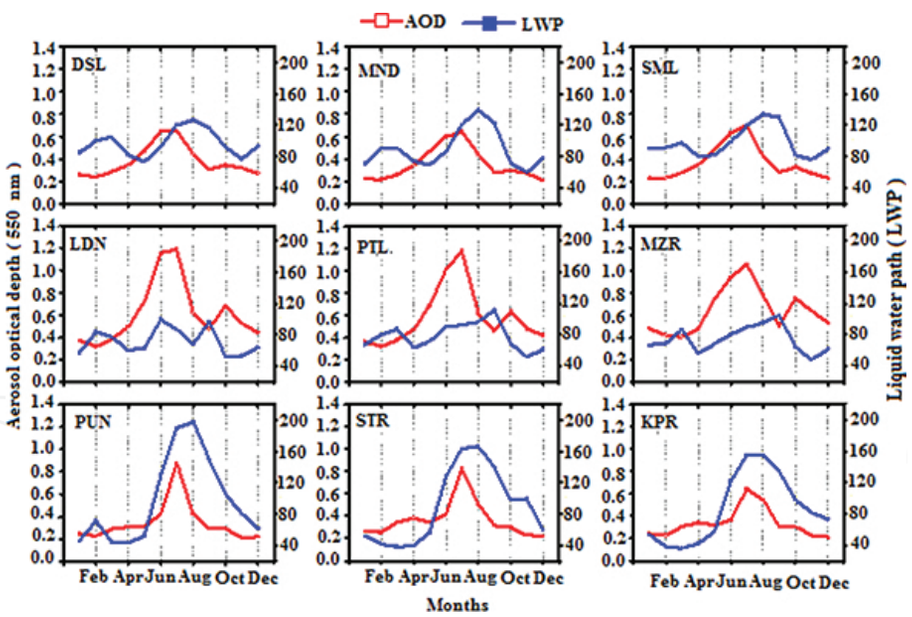

Figure 7. Monthly mean composite plots of AOD and LWP at the selected stations in the Western Himalayan and Deccan Plateau regions during 2000–2010.

Statistical analysis shows that during 2000–2010, about 45 and 11% of the correlation coefficients at the selected stations were significant at 95 and 90%, respectively. During winter, about 56% of the correlation coefficients at the selected stations were consistent with the existing hypothesis (i.e., the negative relationship between AOD and LWP). At the majority of the

stations, during pre-monsoon, negative correlations between AOD and LWP were found to be prevalent for about 89% of the cases, out of which 13% were significant at 95% level. In monsoon, about 56% of the correlation coefficients showed an inverse relationship between AOD and CER; of these about 40% correlation coefficients were significant at 95% confidence level. In all, about 67% of correlation coefficients displayed inconsistency with the Twomey effect and about 33% of the correlation coefficients showed consistency with Twomey effect out of which about 33% of the correlation coefficients were significant at 90% level.

4.4.4. Correlation between AOD and water vapor

Atmospheric water vapor content is an important component of the global climate system and plays an important role in the radiation balance of the earth–atmosphere system [47]. It is the basic and crucial component for the cloud formation. Investigation of the possible changes in column water vapor in association with aerosols may be of considerable importance to give insight into the aerosol impact and speed of hydrological cycle [10]. MODIS retrievals provide column water vapor (CWV) in the clear sky and cloudy or above clouds individually. In the present study, we have used CWV above cloud data retrieved from Terra for the period of 2000–2010. The correlation coefficients were determined at each station situated in both Western Himalayan and Deccan Plateau regions during the period 2000–2010. Analysis (shown in **Table 2**) reveals that at higher latitudes, AOD, and WV have strong positive correlation than at lower latitudes. Strong positive correlations were found over DSL (0.74), MND (0.75), SML (0.74), LDN (0.66), PTL (0.71), and MZR (0.67), whereas relatively low correlation was observed over PUN (0.37), STR (0.37), and KPR (0.38).

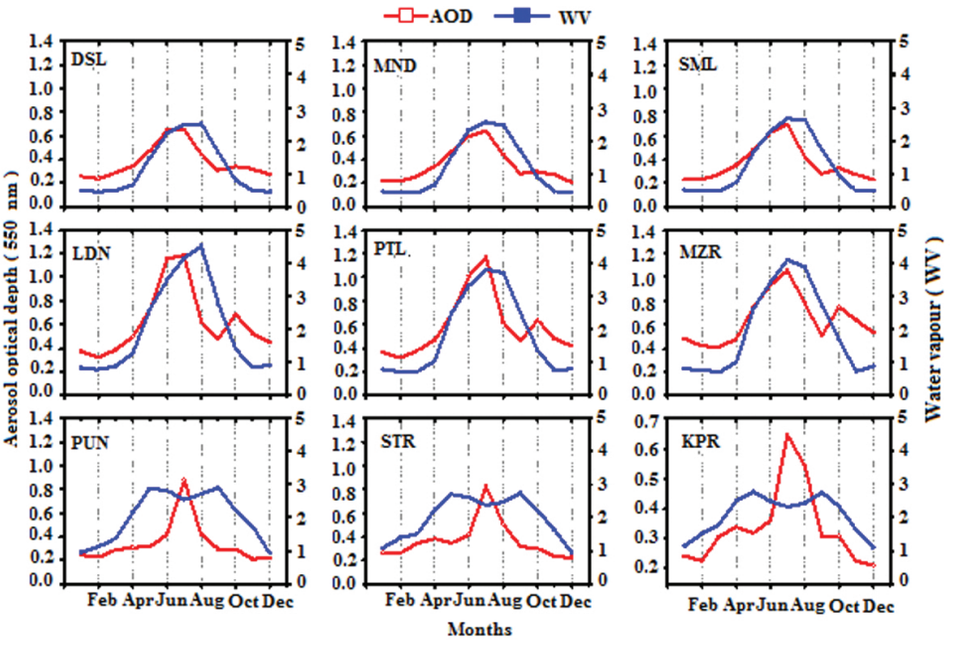

Figure 8. Monthly mean the composite plot of AOD and WV at the selected stations in the Western Himalayan and Deccan Plateau regions during 2000–2010.

http://dx.doi.org/10.5772/65237

The seasonal correlations between AOD and WV (**Table 3**) reveal that AOD and WV have a strong positive correlation (>0.6) over Western Himalayan region and moderate correlation (0.4–0.6) exist at Deccan Plateau region during the pre-monsoon, monsoon, and post-monsoon seasons. There was no significant correlation (<0.32) between AOD and WV during the winter season at all the stations, since the dust aerosols were less common or even absent during winter, consequently, less WV was observed.

Low AOD values in winter, a global feature, is attributed to the removal of aerosols due to monsoon rains and decreased aerosol input due to a colder ground surface. Additionally, the less hygroscopic growth of aerosols due to low WV content may lead to relatively lower AOD values [48]. Also, the decrease in WV with AOD may be a consequence of the increased aerosol loading, since more particles act as cloud condensation nuclei (CCN) followed by an increase in cloud droplet number concentration. Moreover, hygroscopic particles uptake more moisture and this altogether leads to a decrease in WV. It is interesting to note that at the stations PUN, STR, and KPR an abrupt increase in LWP (see Section 4.4.3) was observed during JUN to AUG leading to rapid increase in CER (see Section 4.4.2) and hence the COD. This also supports our hypothesis that WV must have been utilized for the droplet formation thereby decreasing WV. Statistical analysis reveals that at all the selected station's correlation coefficients between AOD and WV during 2000–2010 showed positive AOD-WV relationship, and all the correlation coefficients were significant at 95% level. Seasonally, about 89% of the correlation coefficients at the selected stations evidenced positive correlations in all the seasons. Out of these, about 66 and 16% of correlation coefficients are significant at 95 and 90% confidence level, respectively.

The relation between aerosol and WV has an implication for the radiative forcing both through direct and indirect mechanisms [9]. EL-Askary and Kafatos [49] have found that aerosols cause a reduction in cloud droplet size and hence lead to suppression of the precipitation. The direct effect results in radiation scattering due to an increase in aerosol particle size, accompanied by the uptake of WV. The black cloud episode is comprised mainly of anthropogenic pollutants acting as cloud condensation nuclei leading to the formation of WV cover. The present analysis demonstrates the presence of high WV over locations where high AOD is observed (**Figure 8**).

4.5. Estimation of aerosol indirect effect

The aerosol indirect effect has been estimated using Eq. (1) under fixed LWP as the constraint. For this, magnitudes of LWP are divided into 14 different bins at an interval of 25 g/m^2 viz. 1–25, 25–50, 51–75, 76–100, 101–125, 126–150, 151–175, 176–200, 201–225, 225–250, 251–275, 276–300, 301–325 and 326–350 g/m^2 each. Aerosol indirect effects was estimated seasonally as well as for the entire study period 2000–2010 at each category, and the results are shown in **Figures 9** and **10**, respectively. The two-tailed t-test has also been carried out for determination of the significance of aerosol indirect effect at 90 and 95% confidence levels which are indicated by gray color solid bar and black color solid bar in these figures, respectively.

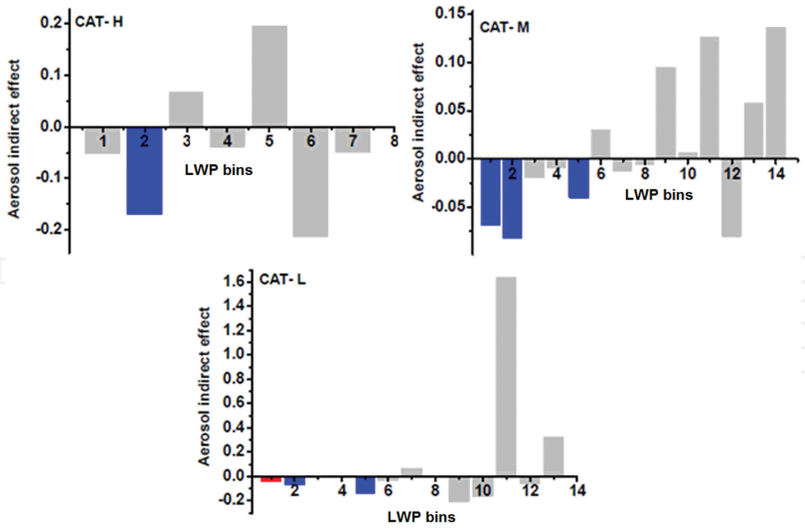

Figure 9. Aerosol indirect effect (AIE) in different LWP bins at different aerosol loading groups H, M, and L during 2000–2010. The range of bin number against LWP is as follows: (1) 1–25; (2) 26–50; (3) 51–75; (4) 76–100; (5) 101–125; (6) 126–150; (7) 151–175; (8) 176–200; (9) 201–225; (10) 226–250; (11) 251–275; (12) 276–300; (13) 301–325 and (14) 326–350 gm^{-2}. (Blue color bars represent AIE significant at 95% of confidence level, Red color bars represent IE significant at 90% of confidence level and rest are less significant).

Figure 9 illustrates the AIE for different LWP bins at each category during 2000–2010. It also reveals that during 2000–2010, the average values of AIE at each category (CAT-H, CAT-M, and CAT-L) were -0.04 ± 0.14, 0.01 ± 0.07, and 0.10 ± 0.48, respectively. About 71% of LWP bins predicted negative AIE at CAT-H, out of which 20% of the LWP bins were found to be statistically significant at 95% level. At CAT-M, about 57% of LWP bins exhibited negative AIE out of which about 38% of the LWP bins were significant at 95% level. AIE at CAT-L was observed to be less prominent as compared to other two categories. About 57% of LWP bins at CAT-L depicted negative AIE out of which 25 and 13% of LWP bins were significant at the level of 95 and 90%, respectively.

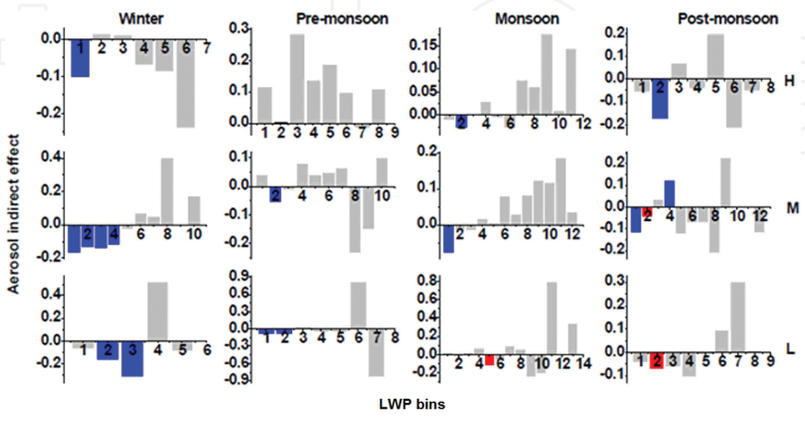

Figure 10. Same as in **Figure 9**, but for seasonal AIE. (Upper panel represents AIE for CAT-H, middle panel shows AIE for CAT-M and lower panel indicates CAT-L.) (Blue color bars represent AIE significant at 95% of confidence level, Red color bars represent IE significant at 90% of confidence level and rest are less significant).

Station	Winter	Pre-monsoon	Monsoon	Post-monsoon
DSL	−0.008 (60%)	0.141 (54.55%)	0.049 (53.85%)	−0.067 (63.64%)
MND	−0.143 (100%)	0.156 (85.71%)	0.118 (75%)	−0.068 (75%)
MSL	−0.045 (71.43%)	0.030 (77.77%)	0.043 (75%)	−0.146 (83.33%)
LDN	0.15 (80%)	0.13 (100%)	−0.023 (75%)	0.07 (80%)
PTL	−0.11 (100%)	0.09 (100%)	0.05 (55.55%)	−0.09 (50%)
MZR	0.10 (60%)	0.23 (83.33%)	0.04 (62.5%)	−0.04 (66.66%)
PUN	−0.121 (100%)	−0.091 (60%)	0.003 (55.56%)	0.024 (50%)
STR	−0.057 (72.72%)	−0.013 (50%)	−0.057 (63.63%)	−0.008 (75%)
KPR	0.038 (60%)	0.106 (83.83%)	−0.250 (60%)	−0.058 (85.71%)

Percentage of cases of positive/negative AIE are given in parenthesis.

Table 4. The seasonal average value of AIE for fixed LWP during 2000–2010.

Seasonal AIE at each category was estimated and is presented in **Figure 10** which shows that during winter, LWP bins at all the three categories demonstrated prominent anti-Twomey (negative AIE) effect, out of which 25, 80, and 50% of the LWP bins were significant at 95% level for CAT-H, CAT-M, and CAT-L, respectively. In pre-monsoon, LWP bins showed positive AIE at CAT-H (86%), and CAT-M (60%) while at CAT-L about 71% of LWP bins elucidated negative AIE. At CAT-H, CAT-M, and CAT-L, in monsoon, the percentage of LWP showing positive AIE were found to be about 60, 75, and 58%, respectively. In post-monsoon, about 71, 70, and 63% of LWP bins showed negative AIE for CAT-H, CAT-M, and CAT-L, respectively. Seasonal means of AIE for fixed LWP at each station were also estimated for the period of 2000–2010, and the results are given in **Table 4**. It reveals that majority of the stations showed the occurrence of negative AIEs during winter (about 67%) and post-monsoon (about 78%), respectively. However, on an average 78 and 67% of the stations revealed the occurrence of positive AIEs in pre-monsoon and monsoon seasons, respectively.

The estimation of AIE at each category and at each station indicates that the sign of AIEs changes with space and time (season). The main reason behind this positive or negative nature of the AIE could be linked with changes in circulation pattern and associated long-range transport of air masses containing different types of aerosols from the different sources [16]. For example, the mixing state of the black carbon, i.e., whether it is located in the interstitial aerosol, or included within the cloud droplets, can influence the resulting cloud droplet population and optical properties and the black carbon aerosol can change sign of the radiative forcing from negative to positive [6]. Additionally, dust plume existing under the cloud can influence the direct, indirect, and semi-direct effect [50]. However, there are several other factors along with meteorological conditions that could contribute to the observed changes in indirect effect [51].

5. Conclusions

MODIS satellite retrievals were used to investigate the spatiotemporal variations of MODIS retrieved aerosol and cloud products over Western Himalayan and Deccan Plateau regions. The data were also employed to study aerosol–cloud interaction and to quantify AIE over these regions for fixed LWP bins. The major conclusions of the present study are as follows:

- The analysis of MODIS retrieved aerosol and cloud products, the interrelation between cloud between aerosol parameters and the estimation of the AIE reveal that the aerosol–cloud relationship as well as AIE changes magnitude and sign both with space and time (season). The change in the atmospheric circulation patterns, in-flux/out-flux of different types of aerosols and varying prevalent meteorological conditions may be the reason behind this positive/negative aerosol indirect effect. Analysis of MODIS retrievals further revealed that the aerosols can change microphysical properties of clouds. However, it is evident that such changes are not determined by aerosols alone as there may be several contributing factors.

- At all the stations, during 2000–2010, the sign of AE-AOD correlation exhibited spatiotemporal variability. During winter, AE was positively correlated with AOD while during monsoon the correlation was negative with 95% of significance level at all the stations. In pre-monsoon, the majority of the stations (78%) showed inverse AE-AOD relationship, out of which about 86% of the correlations were significant at 95% confidence level. The changeover in the sign of AE-AOD correlation may be attributed to the hygroscopic growth of the aerosol particles producing a significant shift in aerosol size spectrum which in turn can substantially influence the magnitude of the AE.

- Monthly variation of AOD and LWP for the study period and their seasonal correlation analysis points out that the sign of correlation (negative/positive) changes from season to season and place to place indicating spatiotemporal variability in these correlations. Reduction in LWP with AOD during winter, pre-monsoon, monsoon, and post-monsoon seasons may be attributed to the warming of the clouds due to the dust aerosols. Dust aerosols absorb the incoming solar radiation resulting into increase in cloud layer temperature, thereby enhancing evaporation of cloud droplets leading to the reduction of LWP, i.e., the so-called semi-direct effect.

- Estimated values of AIE showed that the average values of AIE during 2000–2010, at each category (CAT-H, CAT-M, and CAT-L) were -0.04 ± 0.14, 0.01 ± 0.07, and 0.10 ± 0.48, respectively. About 57–71% of LWP bins revealed negative AIE at each category. During winter, prominent anti-Twomey effect (with 25–80% of significance level) was observed in all the three categories. In pre-monsoon, 86% (at CAT-H) and 60% (at CAT-M) of LWP bins showed positive AIE while about 71% (at CAT-L) of LWP bins exhibited negative AIE values.

Author details

Sandeep R. Varpe[1,3], Gajanan R. Aher[1*], Amol R. Kolhe[1,2] and Sanjay D. More[4]

*Address all correspondence to: aher.g.r@gmail.com

1 Physics Department, Nowrosjee Wadia College, Pune, India

2 Department of Physics, Savitribai Phule Pune University, Pune, India

3 International Institute of Information Technology, Hinjewadi, Pune, India

4 Department of Atmospheric and Space Sciences, University of Pune, Pune, India

References

[1] Tai APK, Mickley LJ, Jacob DJ. Correlations between fine particulate matter (PM2.5) and meteorological variables in the United States: implications for the sensitivity of PM2.5 to climate change. Atmospheric Environment. 2010; 44: 3976–3984.

[2] Lee SS, Penner JE. Dependence of aerosol-cloud interactions in stratocumulus clouds on the liquid-water path. Atmospheric Environment. 2011; 45: 6337–6346.

[3] Satheesh SK, Moorthy KK. Radiative effects of natural aerosols: a review. Atmospheric Environment. 2005; 39: 2089–2110.

[4] Kaufman YJ, Boucher O, Tanre D, Chin M, Remer LA, Takemura T. Aerosol anthropogenic component estimated from satellite data. Geophysical Research Letters. 2005; 32: L17804.

[5] Sundstrom AM, Arola A, Kolmonen P, Xue Y, de Leeuw G, Kulmala AM. On the use of satellite remote-sensing approach for determining aerosol direct radiative effect over land: a case study over China. Atmospheric Chemistry and Physics. 2015; 15: 505.

[6] Ramanathan V, Crutzen PJ, Kiehl JT, Rosenfeld D. Aerosols, climate and the hydrological cycle. Journal of Geophysical Research. 2001; 294: 2119–21124.

[7] Kaufman YJ, Koren I. Smoke and pollution aerosol effect on cloud cover. Science. 2006; 313: 655–658.

[8] Niu F, Li Z. Systematic variations of cloud top temperature and precipitation rate with aerosols over the global tropics. Atmospheric Chemistry and Physics. 2012; 12: 8491–8498.

[9] Houghton JT. et al editors. Climate Change. The scientific basis: contribution of working group I to the third assessment report of the Intergovernmental Panel on Climate Change (IPCC). Cambridge University Press, Cambridge (UK); 2001: 525–582.

[10] Myhre G, Stordal F, Johnsrud M, Kaufman YJ, Rosenfeld D, Storelvmao T, Kristjansson JE, Berntsen TK, Myhre A, Isaksen ISA. Aerosol-cloud interaction inferred from MODIS satellite data and aerosol global models. Atmospheric Chemistry and Physics. 2007; 7: 3081–3101.

[11] Penner JE, Dong XQ, Chen Y. Observational evidence of a change in radiative forcing due to the indirect aerosol effect. Nature. 2004; 427(6971): 231–234.

[12] Balakrishnaiah G, Raghavendra Kumar K, Suresh Kumar Reddy B, Rama Gopal K, Reddy RR, Reddy LSS, Nazeer Ahammed Y, Narasimhulu K, Krishnamoorthy K, Suresh Babu S. Analysis of optical properties of atmospheric aerosols inferred from spectral AODs and Angstrom wavelength exponent. Atmospheric Environment. 2011; 45: 1275–1285.

[13] Rosenfeld D, Lohmann U, Raga GB, O'Dowd CD, Kulmala M, Fuzzi S, Reissell A, Andreae MO. Flood or drought: how do aerosols affect precipitation. Science. 2008; 321: 1309–1313.

[14] Andreae MO, Rosenfeld D, Artaxo P, Costa A, Frank AGP, Longo KM, Silva-Dias MAF. Smoking rain clouds over the Amazon. Science. 2004; 303: 1337–1342.

[15] Ten Hoeve JE, Remer LA, Jacobson MZ. Impacts of water vapor/aerosol loading trends and land cover on aerosol microphysical and radiative effects on clouds during the Amazon biomass burning season. Atmospheric Chemistry and Physics (Discussions). 2010; 10: 24919–24960.

[16] Panicker AS, Pandithurai G, Dipu S. Aerosol indirect effect during successive contrasting monsoon seasons over Indian subcontinent using MODIS data. Atmospheric Environment. 2010; 44: 937–943.

[17] Lohmann U, Feichter J. Global indirect aerosol effects: a review. Atmospheric Chemistry and Physics. 2005; 5: 715–737.

[18] Storelvmo T, Kristjansson JE, Myhre G, Johnsrud M, Stordal F. Combined observational and modeling based study of the aerosol indirect effect. Atmospheric Chemistry and Physics. 2006; 6: 3583–3601.

[19] Ten Hoeve JE, Jacobson MZ, Remer LA. Comparing results from a physical model with satellite and *in situ* observations to determine whether biomass burning aerosols over the Amazon brighten or burn off clouds. Journal of Geophysical Research. 2012; 117: D0820319.

[20] Kumar A. Variability of aerosol optical depth and cloud parameters over North Eastern regions of India retrieved from MODIS satellite data. Journal of Atmospheric and Solar Terrestrial Physics. 2013; 100–101: 34–49.

[21] More SD, Pradeep Kumar P, Gupta P, Devara PCS, Aher GR. Comparison of aerosol products retrieved from AERONET, MICROTOPS and MODIS over a tropical urban city, Pune, India. Aerosol and Air Quality Research. 2013; 13: 107–121.

[22] King MD, Kaufman YJ, Menzel WP, Tanré D. Remote sensing of Cloud, Aerosol, and Water vapor properties from the Moderate Resolution Imaging Spectroradiometer (MODIS). IEEE Transactions on Geoscience and Remote Sensing. 1992; 30(1): 2–26.

[23] Levy RC, Remer LA, Dubovik O. Global aerosol optical properties and application to moderate resolution imaging spectroradiometer aerosol retrieval over land. Journal of Geographical Research. 2007; 112: D13210.

[24] King MD, Menzel WP, Kaufman YJ, Tanre D, Gao BC, Platnick S, Ackerman SA, Remer LA, Pincus R, Hubanks PA. Cloud and aerosol properties, precipitable water, and profiles of temperature and humidity from MODIS. IEEE, Transactions on Geoscience and Remote Sensing. 2003; 41: 442–458.

[25] Remer LA, Kaufman YJ, Tanre D, Matoo S, Chu DA, Martins JV, Li RR, Ichoku C, Levy RC, Kleidman RG, Eck TF, Vermote E, Holben BN. The MODIS aerosol algorithm, products, and validation. Journal of Atmospheric Sciences. 2005; 62: 947–973.

[26] Feingold G, Eberhard WL, Veron DE, Previdi M. First measurements of the Twomey indirect effect using ground-based remote sensors. Geophysical Research Letters. 2003; 30: 1287.

[27] Gautam R, Liu Z, Singh RP, Hsu NC. Two contrasting dust-dominant periods over India observed from MODIS and CALIPSO data. Geophysical Research Letters. 2009; 36: L06813.

[28] Prasad AK, Singh RP, Singh AA. Variability of aerosol optical depth over Indian subcontinent using MODIS data. Journal of the Indian Society of Remote Sensing. 2004; 32(4): 313–316. http://home.iitk.ac.in/~ramesh/jisrs/jisrs.html.

[29] Ramchandran S, Cherian B. Regional and seasonal variations in aerosol optical characteristics and their frequency distributions over India during 2001-2005. Journal of Geophysical Research. 2008; 113: D08207.

[30] Tripathi SN, Dey S, Chandel A, Shrivastava S, Singh RP, Holben BN. Comparison of MODIS and AERONET derived aerosol optical depth over the Ganga basin, India. Annals of Geophysics. 2005; 23: 1093–1101.

[31] Dey S, Tripathi SN, Singh RP, Holben BN. Influence of dust storms on the aerosol optical properties over the Indo-Gangetic basin. Journal of Geophysical Research. 2004; 109: D20211.

[32] Balakrishnaiah G, Kumar KR, Reddy BS, Gopal KR, Reddy RR, Reddy LSS, Swamulu C, Ahammed YN, Narasimhulu K, Krishnamoorthy K, Babu SS. Spatio-temporal variation in aerosol optical depth and cloud parameters over Southern India retrieved from MODIS satellite data. Atmospheric Environment. 2012; 47: 435–445.

[33] Mishra A, Klingmueller K, Fredj E, Lelieveld J, Rudich Y, Koren I. Radiative signature of absorbing aerosol over the eastern Mediterranean basin. Atmospheric Chemistry and Physics. 2014; 14: 7213–7231.

[34] Dubovik O, Sinyuk A, Lapyonok T, Sinyuk A, Mishchenko MI, Yang P, Eck TF, Volten H, Munoz O, Veihelmann B, van der Zander WJ, Sorokin M, Slutsker I. Application of light scattering by spheroids for accounting for particle non-sphericity in remote sensing of desert dust. Journal of Geophysical Research. 2006; 111: D11208. doi: 10.1029/2005JD006619.

[35] Aher GR, Pawar GV, Gupta P, Devara PCS. Effect of a major dust storm on optical, physical, and radiative properties of aerosols over coastal and urban environments in Western India. International Journal of Remote Sensing. 2014; 35: 871–903. doi: 10.1080/01431161.2013.873153.

[36] Graf HF. The complex interaction of aerosols and clouds. Science. 2004; 303: 1309–1311.

[37] Li Z, Niu F, Fan J, Liu Y, Rosenfield D, Ding Y. Long-term impacts of aerosols on the vertical development of clouds and precipitation. Nature Geoscience. 2011; 4(12): 888–894.

[38] Wright ME, Atkinson DB, Ziemba L, Griffin R, Hiranuma N, Sarah B, Lefer B, Flynn J, Perna R, Rappengluck B, Luke W, Kelley P. Extensive aerosol optical properties and aerosol mass related measurements during TRAMP/Tex AQS2006-Implications for PM compliance and planning. Atmospheric Environment. 2010; 44: 4035–4044.

[39] Philipp F, Markus F, Fritzsche L, Petzold A. Measurement of ultrafine aerosol size distributions by a combination of diffusion condensation particle counters. Journal of Aerosol Science. 2006; 37: 577–597.

[40] Walcek CJ. Cloud cover and its relationship to other meteorological factors during a springtime midlatitude cyclone. Monthly Weather Review. 1994; 120:1021–1035.

[41] Kaskaouties DG, Kharol SK, Sinha PR, Singh RP, Kambezidis HD, Sharma AR, Badarinath KVS. Extremely large anthropogenic-aerosol contribution to total aerosol load over the Bay of Bengal during the winter season. Atmospheric Chemistry and Physics. 2011; 11: 7079–7117.

[42] Chou MD, Chan PK, Wang M. Aerosol radiative forcing derived from Sea WiFS-retrieved aerosol optical properties. Journal of the Atmospheric Sciences. 2002; 59: 748–757.

[43] Indira G, Bhaskar BV, Krishnaswamy M. The Impact of aerosol optical depth impacts on rainfall in two different monsoon periods over Madurai, India. Aerosol and Air Quality Research. 2013; 13: 1608–1618.

[44] Yuan T, Li Z, Zhang R, Fan J. Increase of cloud droplet size with aerosol optical depth: an observation and modeling study. Journal of Geophysical Research. 2008; 113: D04201.

[45] Bhawar RL, Devara PCS. Study of successive contrasting monsoons (2001-2002) in terms of aerosol variability over a tropical station Pune, India. Atmospheric Chemistry and Physics. 2010; 10: 29–37.

[46] Huang J, Lin B, Minnis P, Wang T, Wang X, Hu Y, Yi Y, Ayers JK. Satellite-based assessment of possible dust aerosols semi-direct effect on cloud water path over East Asia. Geophysical Research Letters. 2006; 33: L19802.

[47] Peixoto JP, Oort AH. The Atmospheric Branch of the Hydrological Cycle and Climate. Street-Perrott A, Beran M, Ratcliff R, editors. Variations in the Global Water Budget. Springer Netherlands (D. Reidel Publishing Company) 1983. 5–65. DOI: 10.1007/978-94-009-6954-4_2.

[48] Ranjan RR, Joshi HP, Iyer KN. Spectral variation of total column aerosol optical depth over Rajkot: a tropical semi-arid Indian station. Aerosol and Air Quality Research. 2007; 7: 33–45.

[49] El-Askary H, Kafatos M. Dust storm and black cloud influence on aerosol optical properties over Cairo and the Greater Delta Region, Egypt. International Journal of Remote Sensing. 2008; 29(24): 7199–7211. doi:10.1080/01431160802144179.

[50] Su J, Huang J, Fu Q, Minnis P, Ge J, Bi J. Estimation of Asian dust aerosol effect on cloud radiation forcing using Fu-Liou radiative model and CERES measurements. Atmospheric Chemistry and Physics. 2008; 8: 2763–2771.

[51] Yu H, Fu R, Dickinson RE, Zhang Y, Chen M, Wang H. Inter-annual variability of smoke and warm cloud relationships in the Amazon as inferred from MODIS retrievals. Remote Sensing of Environment. 2007; 111(4): 435–449.

IntechOpen